SUPPLEMENTAL FIGURES AND LEGENDS

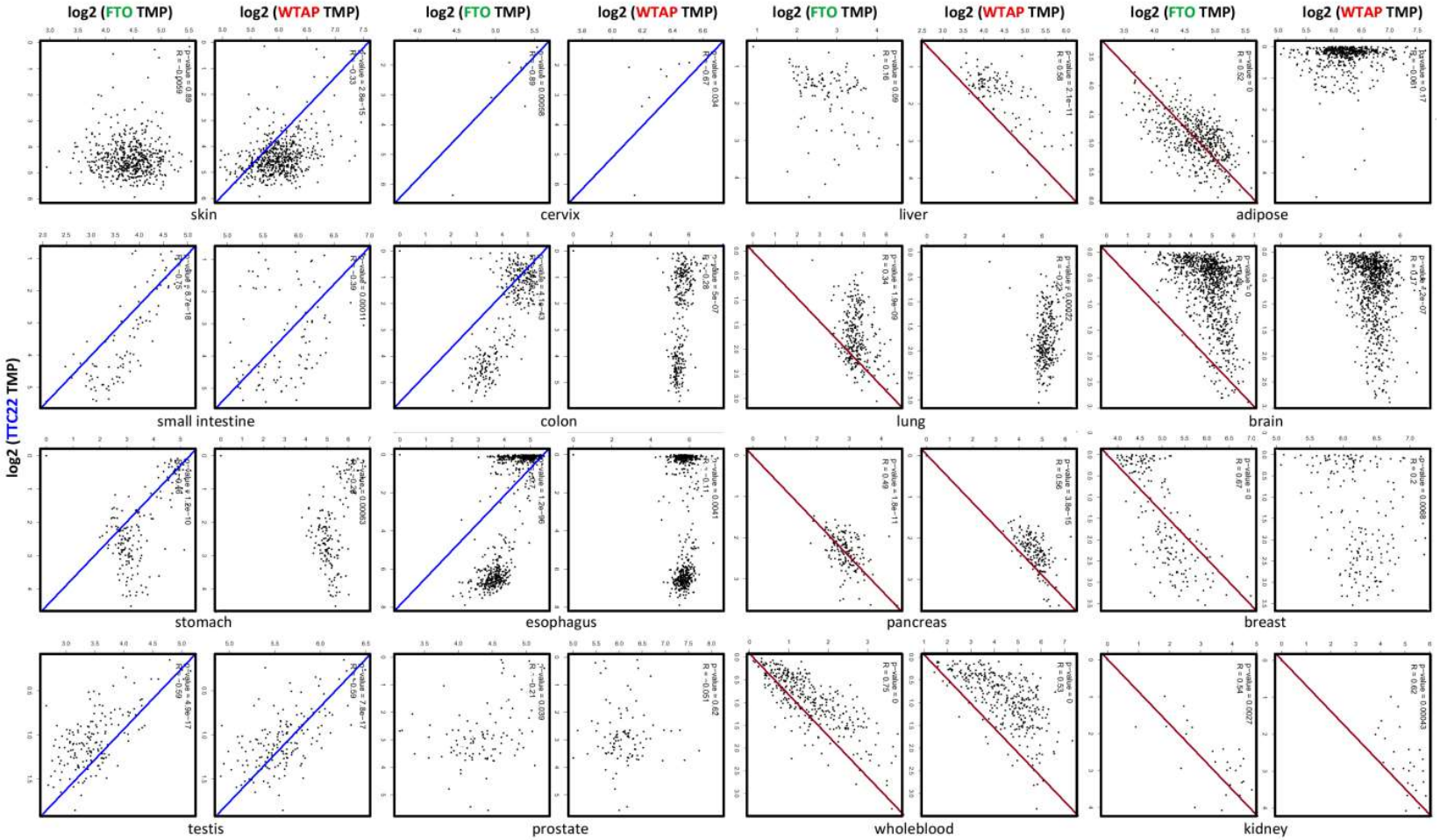

Figure S1. Cooccurrence of *TTC22* expression with *WTAP* and *FTO* expression in various normal human tissues from 570 subjects in the GTEx project [15, 16]. These images were adapted from charts downloaded from the Gene Expression Profiling Interactive Analysis website (gepia.cancer-pku.cn/index.html). The exact coexpression coefficients (R) and p values are labeled. Red and blue lines: R>+0.3 (correlated positively) and R<-0.3 (correlated reversely), respectively.

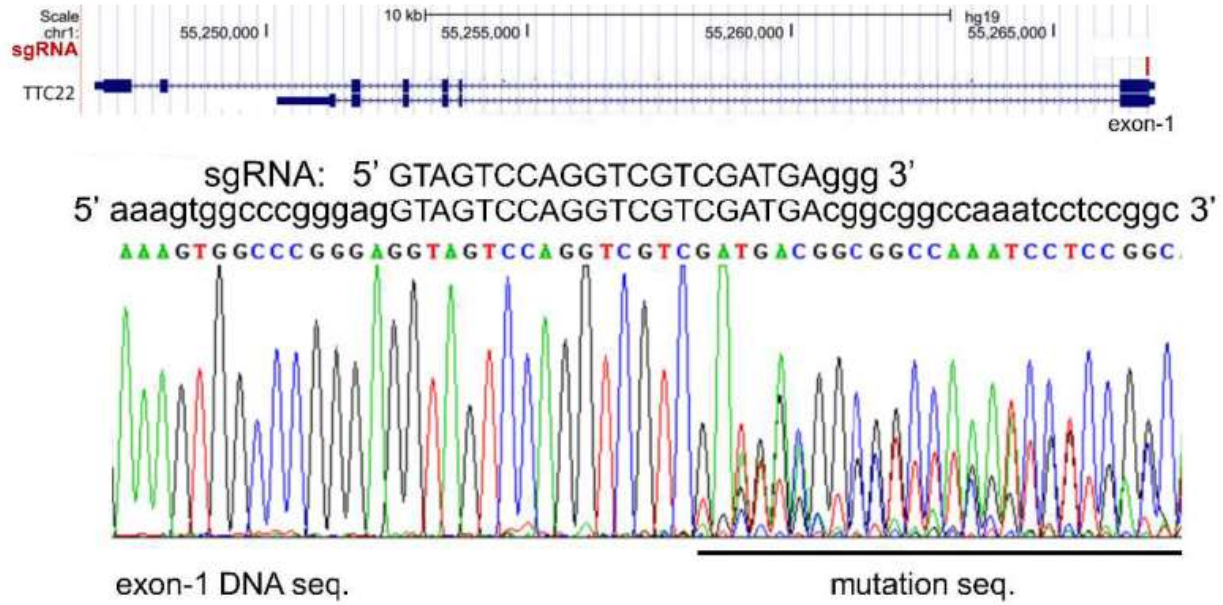

Figure S2. Knockout of the *TTC22* gene by CRISPR/Cas9 using a guide RNA targeting exon 1. Sequences of the single guide RNA (sgRNA) and matched fragment in *TTC22* exon-1 are listed. The knockout status of the target DNA sequence in exon-1 in Caco-2 cells was confirmed by PCR sequencing.

Figure S3. Gene ontology biological process analyses for differentially expressed genes in TTC22-KO and TTC22-KD Caco-2 cells in meRIP-seq analysis. (**A** and **B**) KEGG enrichment analysis of genes downregulated and upregulated by TTC22-KO; (**C** and **D**) KEGG enrichment analysis of genes downregulated and upregulated by TTC22-KD; hallmark processes, q value < 0.01

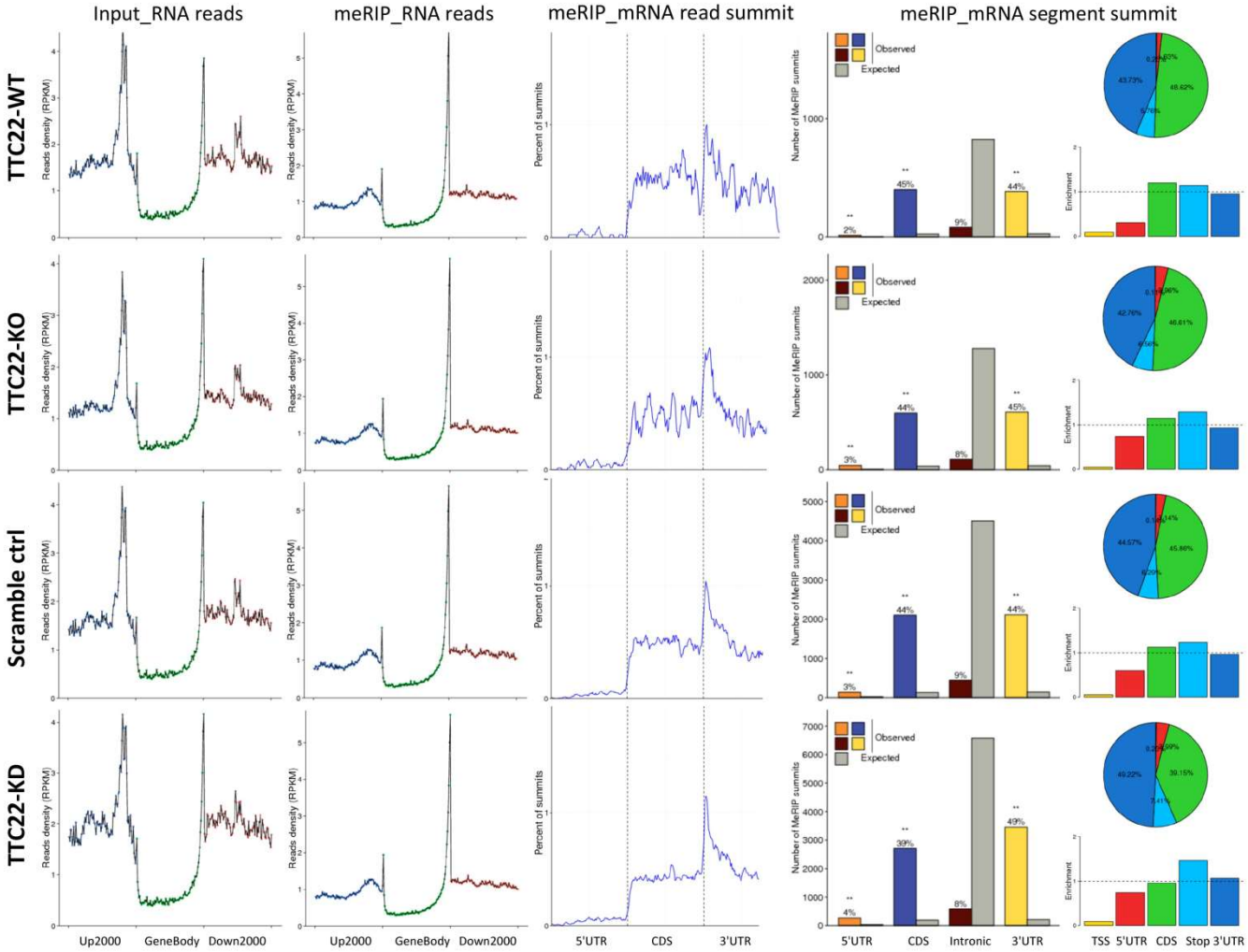

Figure S4. Density distributions of m6A peaks across global RNA and mRNA transcripts in Caco-2 cells with and without TTC22-KD/KO in meRIP-seq analysis. The number of m6A reads within regions of the 5' untranslated region (5'UTR), coding region (CDS), 3' untranslated region (3'UTR), transcription start site (TSS), and stop codon (Stop) are displayed on the right charts. The input RNA-seq analysis is displayed on the left as the paired reference for each cell treatment.

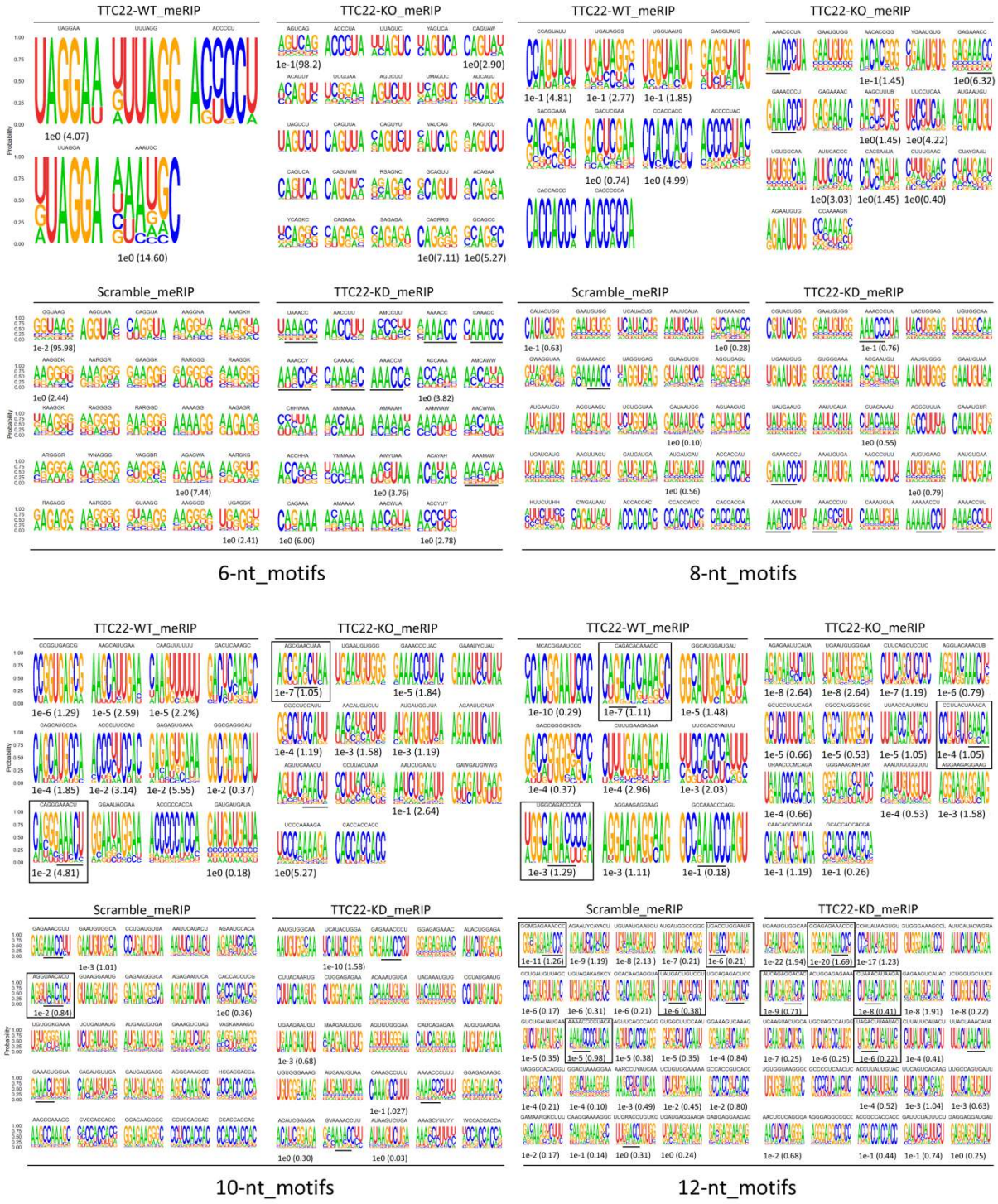

Figure S5. Significant consensus motifs detected in Caco-2 cells with and without TTC22-KO/KD in the meRIP-seq analysis. The 6-nt, 8-nt, 10-nt, and 12-nt motifs are listed for these cells. The p-value and percent of the number of motif to the number of total target sequences with the motif (%) are listed for each enriched motif. Typical m6A consensus DRACH (5'-3'; D=A/G/U, R=A/G, H=A/C/U) motifs are underlined. Significant DRACH motifs are highlighted with black rectangles. These motifs in m6A peaks within mRNA were calculated by Homer software. The number of total target sequences with motif/total background sequences with motif were 543/261875 for TTC22-WT cells, 762/231167 for TTC22-KO cells, 2868/253145 for Scramble cells, and 3665/250800 for TTC22-KD cells.

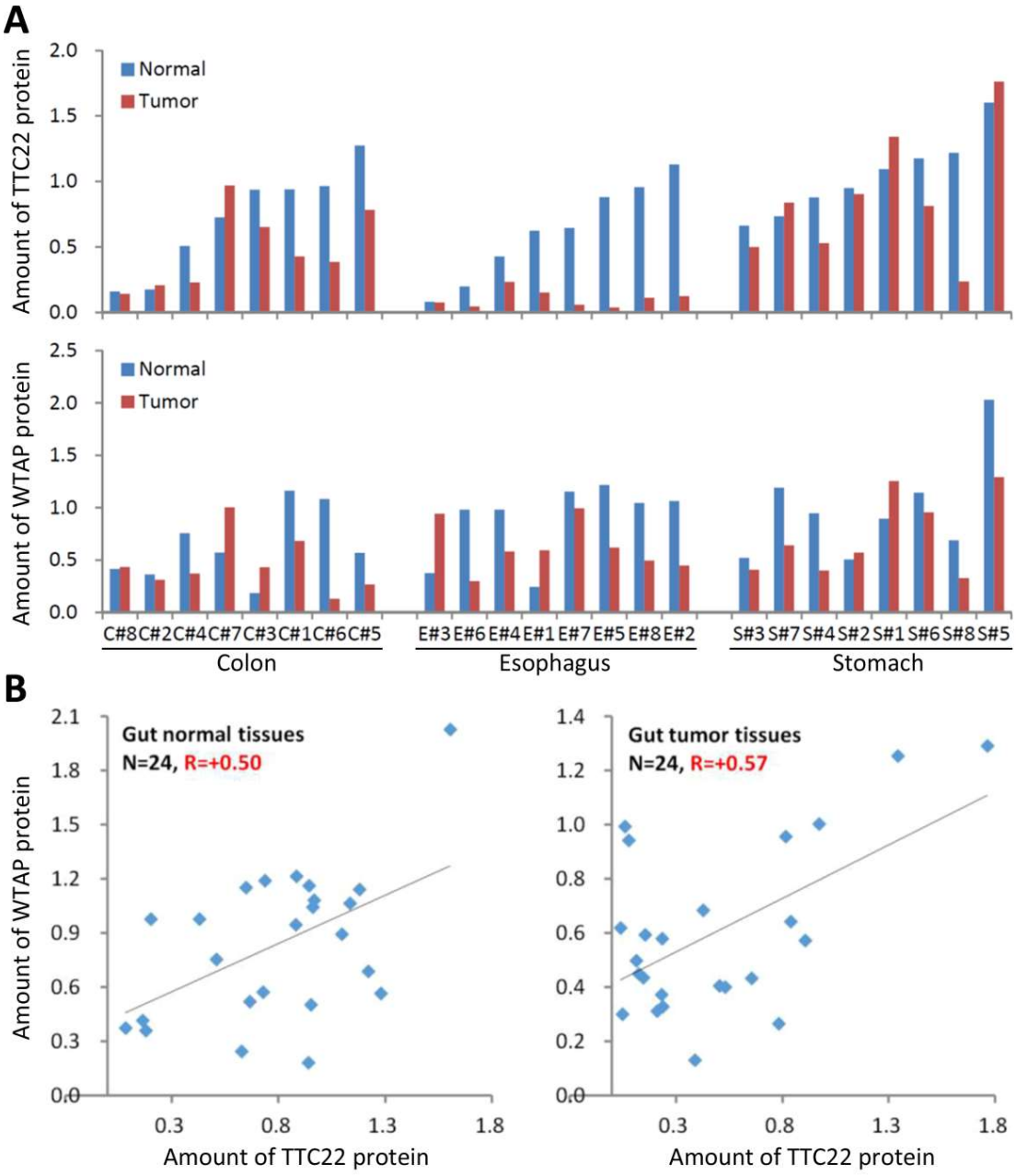

Figure S6. The amounts of WTAP and TTC22 proteins in cancer tissue and paired normal tissue samples from 8 patients, respectively. (**A**) Band densities corresponding to target proteins were scanned and normalized to the GAPDH reference values in Western blot analysis. (**B**) Correlation between WTAP and TTC22 protein expression levels in these 24 cancer and paired normal samples. Both the trend line and coexpression coefficient (R) are also shown.

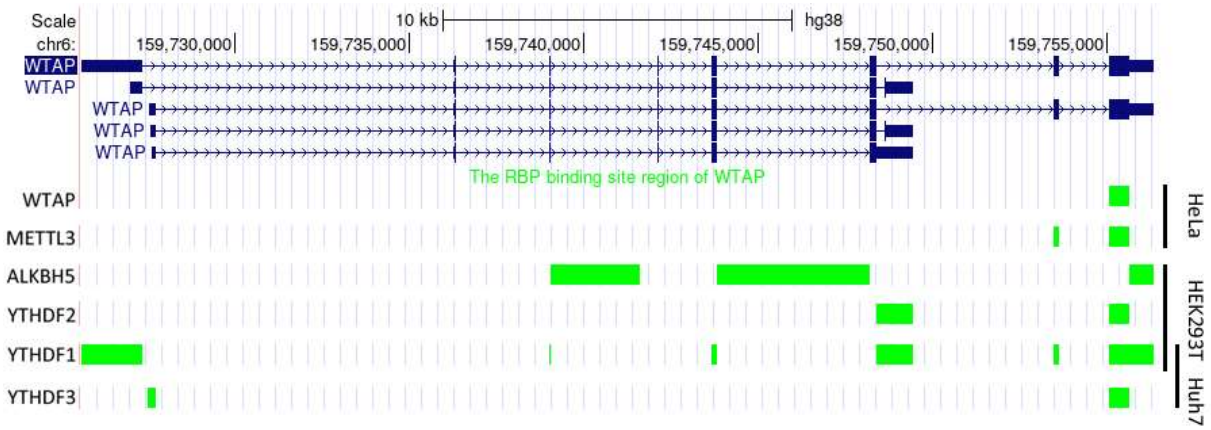

Figure S7. Graphical presentation of *WTAP* transcripts in CLIP-seq. Cross-linking and immunoprecipitation (CLIP)-seq datasets (GSE46705 and GSM1135011 for WTAP; GSE46705 and GSM1135006 for METTL3; GSE38201 and GSM936506 for ALKBH5; GSE78030 and GSM2064706 for YTHDF2; GSE78030 and GSM2064705 for YTHDF1; GSE83438 and GSM2203040 for YTHDF3) for RNAs binding to WTAP, METTL3, ALKBH5, or YTHDF1-3 in HeLa, HEK293T, and Huh7 cells (adapted from the POSTAR3 website, http://rmvar.renlab.org)[17-19]

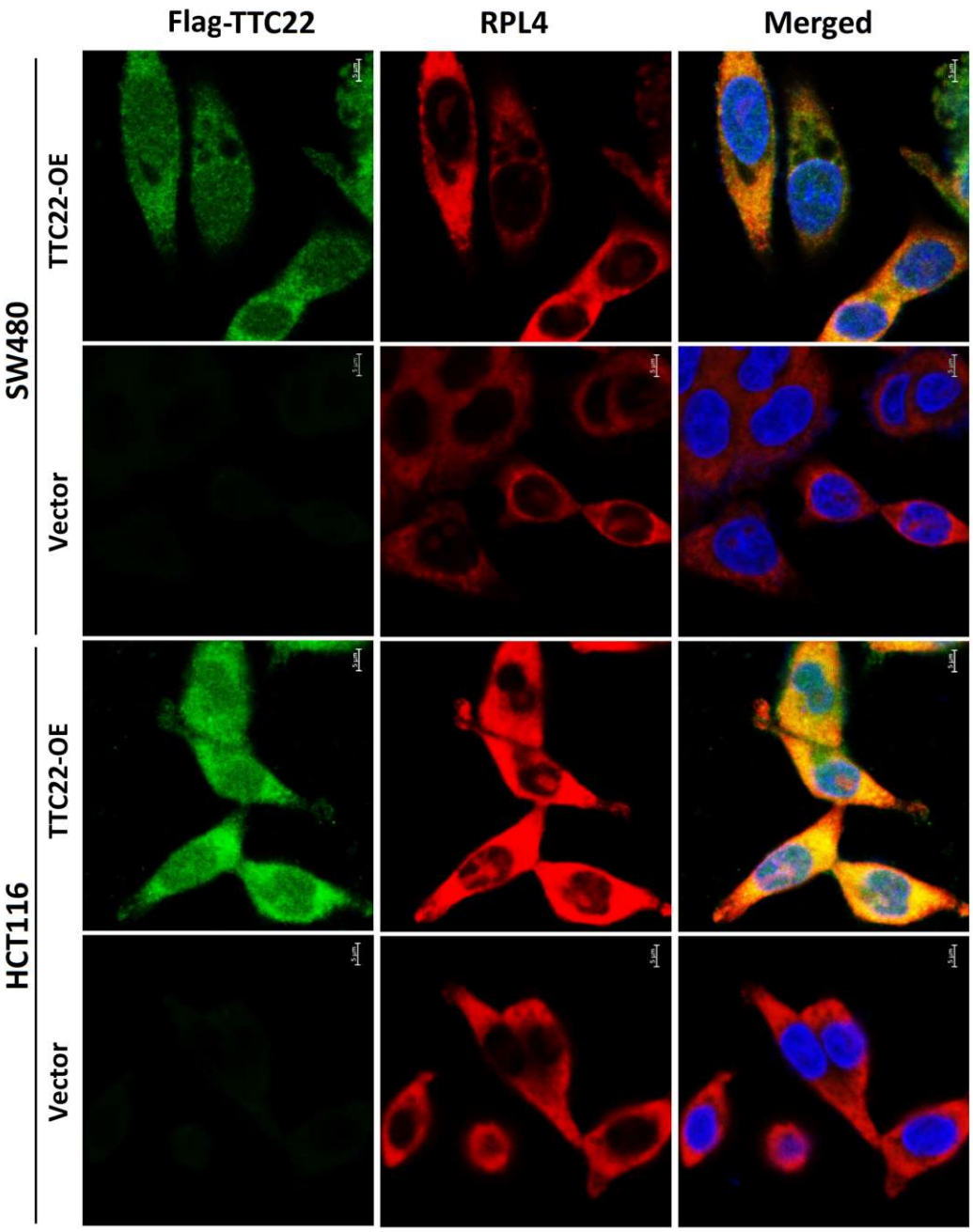

Figure S8. Images of indirect immunofluorescence cell staining and confocal microscopy analysis of overexpressed TTC22-Flag (labeled with an anti-Flag antibody) and endogenous RPL4 (labeled with an anti-RPL4 antibody) in HCT116 and SW480 cells with and without TTC22-OE

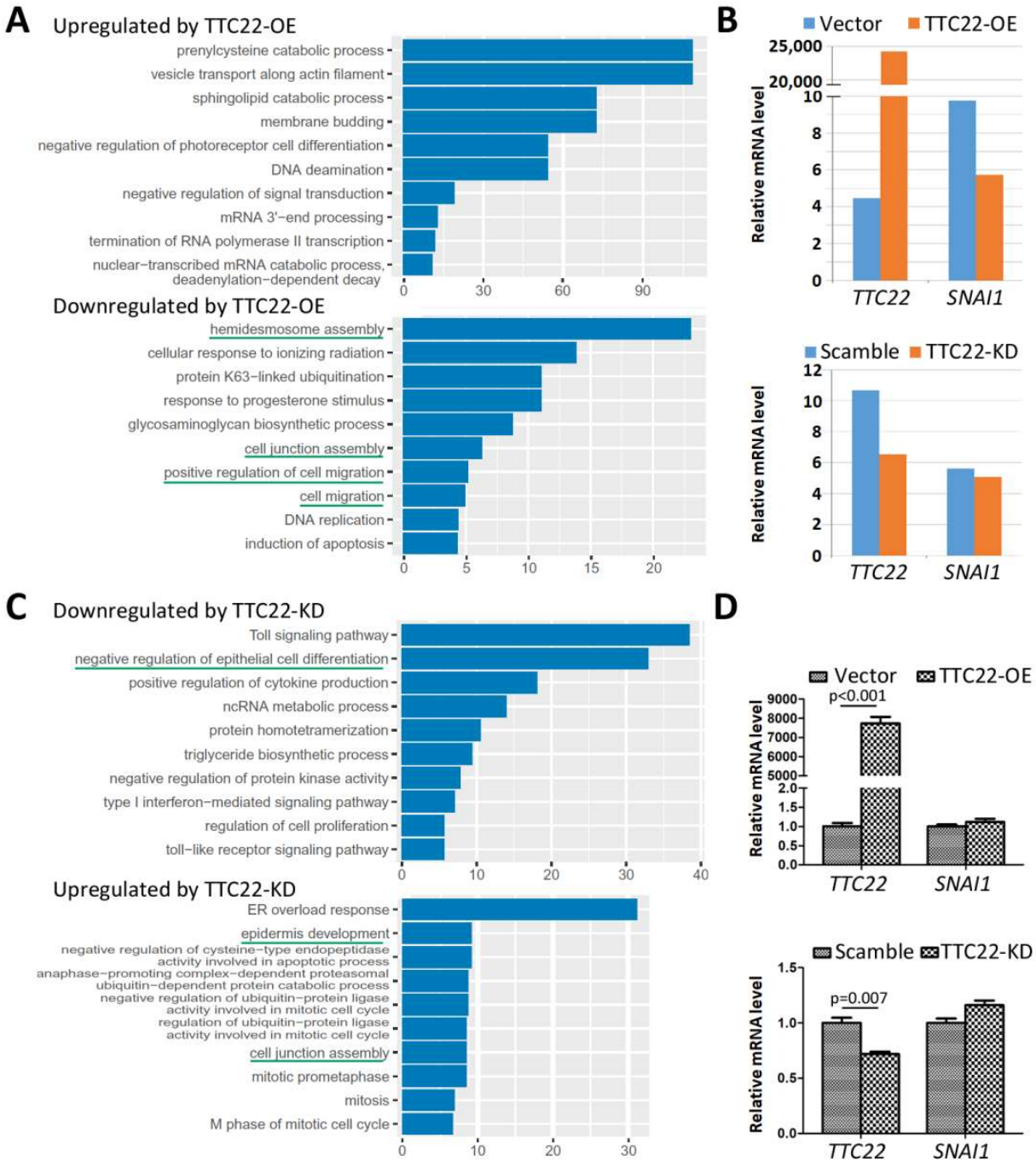

Figure S9. Gene ontology analysis of differentially expressed genes identified by RNA-seq in HCT116 cells with different *TTC22* expression changes. (**A** and **B**) The results of Gene Ontology biological process analysis of TTC22-OE and TTC22-KD HCT116 cells. (**C**) The relative levels of *TTC22* and *SNAI1* mRNAs in TTC22-OE and TTC22-KD HCT116 cells in the RNA-seq data. (**D**) The relative levels of *TTC22* and *SNAI1* mRNAs in TTC22-OE and TTC22-KD HCT116 cells in qRT-PCR analysis (n=3).

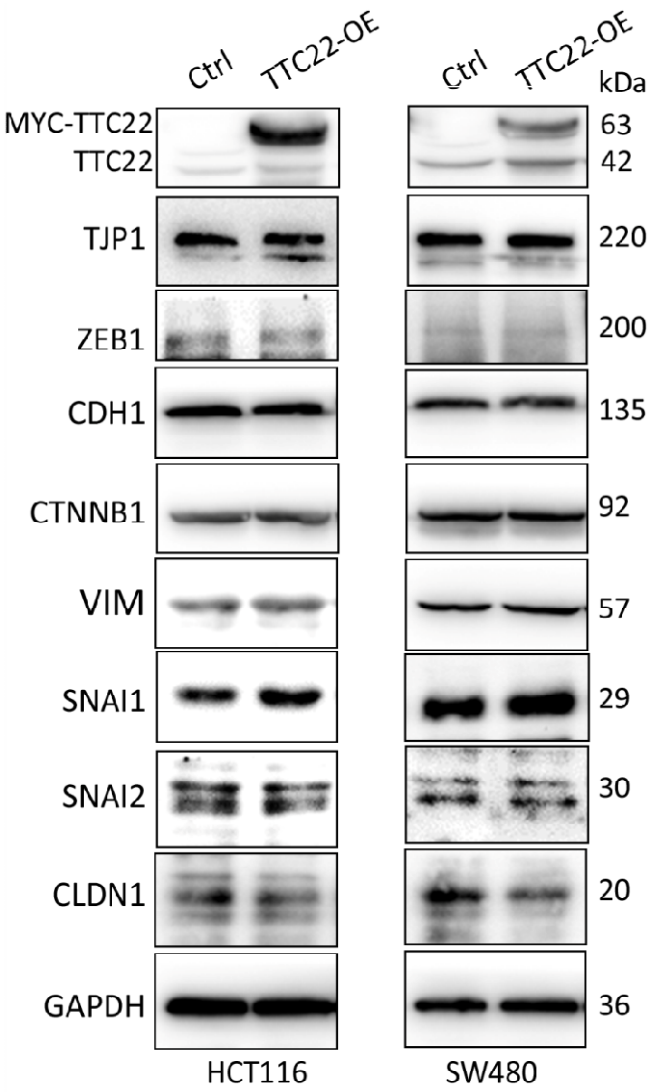

Figure S10. Comparison of the expression status of EMT-related genes in colon cancer cell lines with and without transient TTC22-OE at 48 hrs post transfection, as determined by Western blot analysis

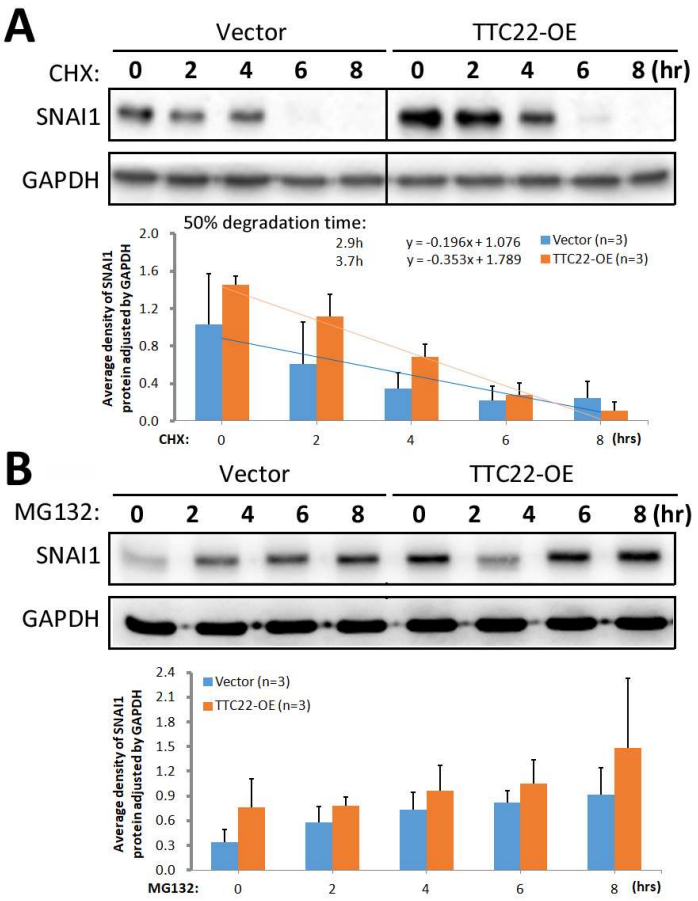

Figure S11. SNAI1 expression changes in TTC22-OE HCT116 cells as determined by Western blot analysis. (**A**) Cells were co-treated with the ribosomal inhibitor CHX (final concentration, 50 μg/mL; top); the half-life of SNAI1 protein in cells with and without TTC22-OE was calculated with the trend line formula: 2.9 and 3.7 hrs in the Vector and TTC22-OE cells; (**B**) proteasome inhibitor MG132 (10 mM; middle). The average GAPDH-normalized band density (ratio) for the SNAI1 protein lanes in three biologically independent experiments is also shown in the charts under the images.

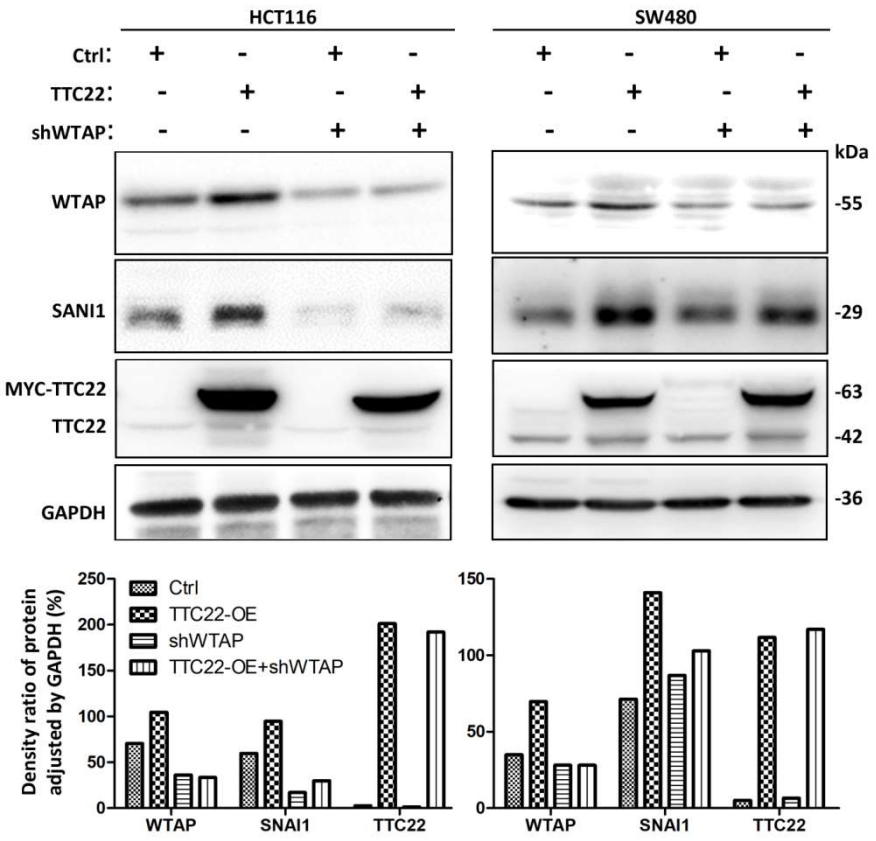

Figure S12. Effect of stable knockdown of WTAP expression by shRNA on SNAI1 expression in HCT116 and SW480 cells, as determined by Western blot analysis

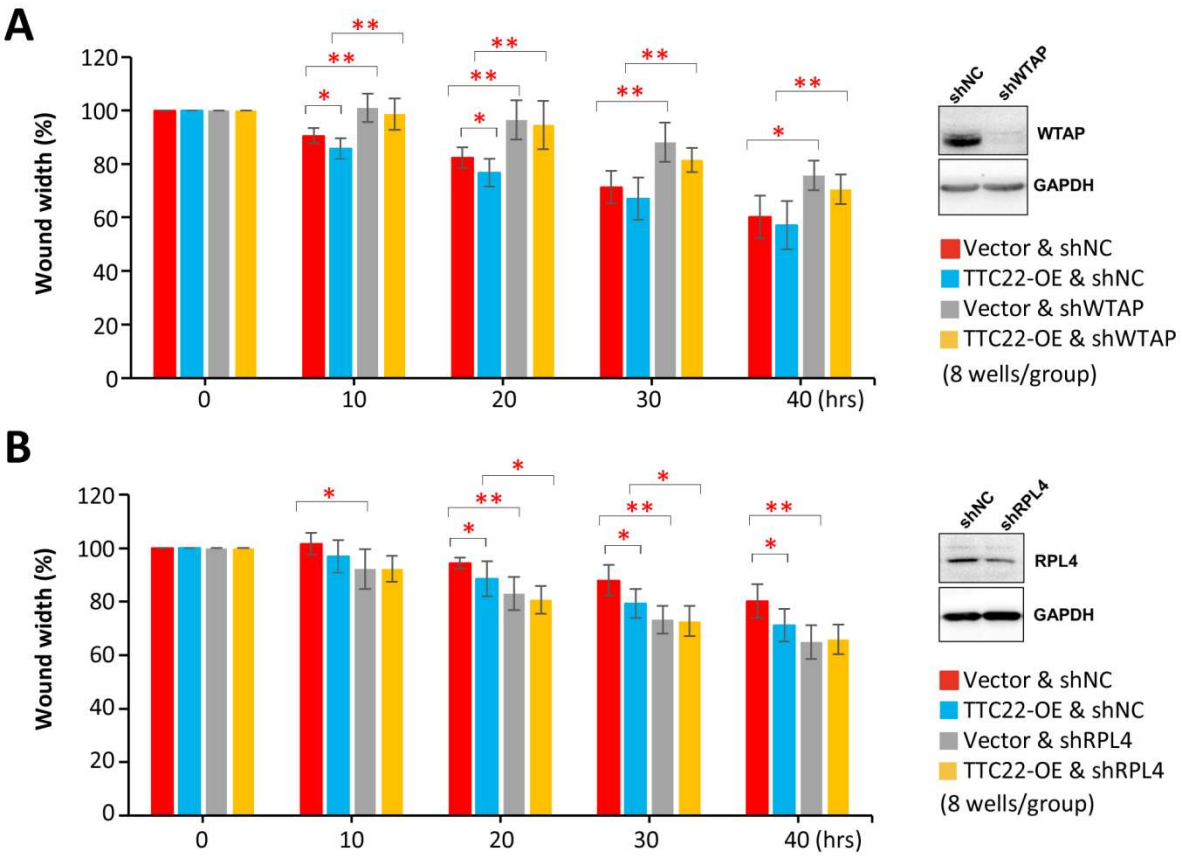

Figure S13. Results of the wound-healing migration assay of HCT116 cells using long-term monitoring with an IncuCyte ZOOM live-cell imaging system. (**A**) Effect of shRNA stable *WTAP* knockdown (shWTAP) on *TTC22*-enhanced cell migration. (**B**) Effect of shRNA stable knockdown of *RPL4* expression (shRPL4) on the migration of *TTC22*-enhanced cell migration. The amounts of WTAP and RPL4 protein in the shWTAP and shRPL4 and control (shNC) cells were determined by Western blot analysis and inserted on the right sides. */**: $p<0.05/0.01$